TEKA. COMMISSION OF MOTORIZATION AND ENERGETICS IN AGRICULTURE – 2014, Vol. 14, No.1, 182-190

Helical gear train load capacity criterion

Pavel Nosko[1], Valentin Shyshov[1], Denis Ratov[1], Pavel Fil1, Andrii Lysenko[2]

[1]Volodymyr Dahl East Ukrainian National University,
Molodizhny bl., 20a, Lugansk, 91034, Ukraine,
e-mail: mash_ved@snu.edu.ua, mashved@mail.ru
[2]Luxoft, 225 West 34th St, Ste. 1706/1707, New York, NY 10122
e-mail: andriy.Lysenko@ubs.com

Received January 14.2014: accepted February 05.2014

Summary: In the article, the results of the study on helical gear load capacity increase are represented, and one of the most important criteria of transmission performance is introduced – it is the contact tightness coefficient of active lateral surfaces of gear teeth. The coefficient characterizes the stressed state of helical gear teeth. To build a mathematical model of the teeth stressed state, analytical dependences were derived that uniquely identify the theoretical initial surfaces of helical gears.
The results of the comparative analysis confirm the direct dependence of gear train load capacity on the contact tightness coefficient.
Key words: helical gear, contact tightness coefficient, load capacity criterion, stressed state, objective function, optimization, synthesis.

INTRODUCTION

During the design of crossed-axis helical gears, a forced deviation from the hyperboloid base of initial surfaces affected operating characteristics of such transmissions, as compared to their theoretical potential [11]. Substantial improvement of technical characteristics and transmission competitiveness are possible in case of the hyperbolical axoid as initial surfaces, or surfaces that are less deviated from hyperbolic axoids [16, 11, 10, 8]. The important task arising during the gear design is the defining of geometric parameters values of original profile that could ensure the best value of the objective function, taking into account the qualitative parameters of the performance and load capacity of gear [17, 18, 26]. During the helical gear design, the load distribution in tooth flank and the size of contact area have to be studied for defining the allowable contacting, bending and shearing stresses in tooth.

In machine science, the gear train performance is assessed using quality indicators [11, 15] – the criteria characterizing local kinematic and hydrodynamic phenomena in the teeth contact patch, as well as the load capacity of transmissions.

Contact stress eventually results in tooth fatigue breakdown in the contact patch. This destruction becomes apparent in surface chipping.

We introduce a contact tightness coefficient (K_p) [11, 20, 23], which characterizes the stress state of helical gear tooth:

$$K_p = \frac{S}{S_z}, \tag{1}$$

where: S – surface area of instant contact, S_z – area of the lateral surface of helical hyperboloid gear tooth, K_p coefficient is, to a certain extent, an analogue of K_S coefficient of a comparative stressed state of gear teeth [11].

The physical meaning of the contact tightness coefficient: increase (decrease) of K_p means an increase (decrease) of teeth load capacity and contact strength and, consequently, increase (decrease) in the entire gear durability.

Theoretical initial surfaces of helical gears are one-sheeted hyperboloid of revolution the equations of which are the following:

$$x_m^2 + y_m^2 - tg^2\beta_m z_m^2 = r_m^2, \quad \left(m = \overline{1,2}\right). \qquad (2)$$

Necessary and sufficient set of constraints is applied to geometric parameters of surfaces defined by equation (2):

$$\begin{cases} r_1 + r_2 = a_w, \\ \beta_1 + \beta_2 = \gamma, \\ r_1 ctg\beta_1 = r_2 ctg\beta_2, \\ u_0 = \dfrac{r_1 \cos\beta_1}{r_2 \cos\beta_2}, \end{cases} \qquad (3)$$

where: a_w is the distance between axes, γ is crossing angle of gears, u_0 is reduction ratio, r_1, r_2 are radiuses of the neck of initial hyperboloids, β_1, β_2 are angles of slope of hyperboloid generating lines (Fig. 1).

Solving the system (3) with respect to the geometric parameters of one-sheeted hyperboloids β_1, β_2, r_1, r_2, the following dependences uniquely defining the theoretical initial surfaces of helical gears:

$$\begin{aligned} \beta_1 &= arctg \frac{u_0 \sin\gamma}{1 + u_0 \cos\gamma}, \\ \beta_2 &= \gamma - arctg \frac{u_0 \sin\gamma}{1 + u_0 \cos\gamma}, \\ r_1 &= a_w \frac{(u_0 + \cos\gamma) u_0}{u_0^2 + 2u_0 \cos\gamma + 1}, \\ r_2 &= a_w \frac{1 + u_0 \cos\gamma}{u_0^2 + 2u_0 \cos\gamma + 1}. \end{aligned} \qquad (4)$$

In this paper, the hypothesis is assumed that a real contact patch of helical gears, with sufficient accuracy for solving practical problems, can be represented by an ellipse (Fig. 2, a). This hypothesis is supported by recent studies [11, 7, 13]. The size of an elliptical contact patch depends on the geometrical parameters of the contacting surfaces, the resilience moduli of gear material and normal load on gear teeth.

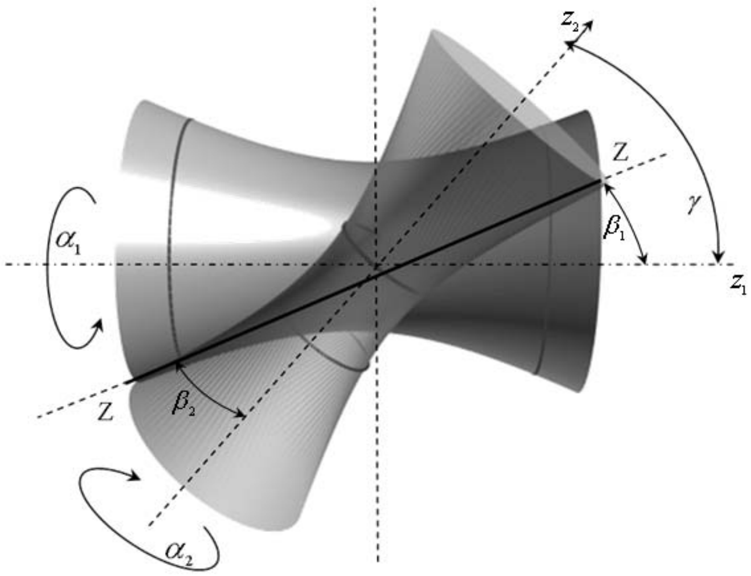

Fig. 1. Surfaces of an one-sheeted hyperboloid of revolution

Normal load P_n is distributed over the entire ellipse area – area of instantaneous contact (Fig. 2, a), that has an area defined according to the formula:

$$S = \pi ab\,, \tag{5}$$

where: a is a major semiaxis of the contact ellipse, b is a minor semiaxis of the contact ellipse.

The equation of the ellipse is

$$\frac{x^2}{a^2} + \frac{y^2}{b^2} = 1\,. \tag{6}$$

Pressure at any point of elliptical area is proportional to the z – applicate of the stressed state semi-ellipsoid (Fig. 2, b):

$$\frac{x^2}{a^2} + \frac{y^2}{b^2} + \frac{z^2}{c^2} = 1\,, \tag{7}$$

where: a, b, c are semi-axes of the stressed state ellipsoid.

On the other hand, the area S_z of a helical tooth flank of a hyperboloid gear is defined by the formula:

$$S_z = LL_a\,, \tag{8}$$

where: L is a tooth length (length of a one-sheet hyperboloid generating line), L_a is an arc length of the lateral surface tooth profile.

Tooth length L is defined by the formula (Fig. 3, a)

$$L = \frac{H}{\cos\beta_n}\,. \tag{9}$$

Since the equation of a one-sheet hyperboloid of rotation looks as follows (2), the height of the hyperboloid (gear rim width) will be equal to:

$$H = 2ctg\beta_n\sqrt{r_t^2 - r_1^2}\,, \tag{10}$$

where: H is a rim width, r_1 is the radius of hyperboloid neck, r_t is the radius of the hyperboloid in the butt, β_n is the slope angle to rotation axis (Fig. 3, a).

The arc length L_a depends on the radius of the profile and the tooth height (Fig. 3, b)

$$L_a = \rho_a\left(arcsin\left(\frac{h_a + y_a}{\rho_a}\right) - arcsin\left(\frac{y_a}{\rho_a}\right)\right). \tag{11}$$

Thereby, the contact tightness coefficient can be defined according to the formula:

$$K_p = \frac{S}{S_z} = $$

$$= \frac{\pi ab\cos\beta_n}{2ctg\beta_n\sqrt{r_t^2 - r_1^2}\,\rho_a\left(arcsin\left(\frac{h_a + y_a}{\rho_a}\right) - arcsin\left(\frac{y_a}{\rho_a}\right)\right)} =$$

$$= \frac{\pi ab\sin\beta_n}{2\rho_a\sqrt{r_t^2 - r_1^2}\left(arcsin\left(\frac{h_a + y_a}{\rho_a}\right) - arcsin\left(\frac{y_a}{\rho_a}\right)\right)}\,. \tag{12}$$

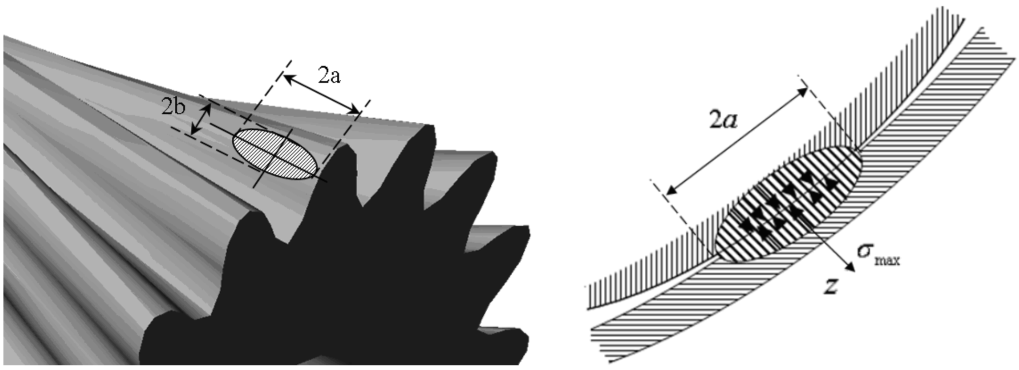

a *b*

Fig. 2. The elliptical contact patch of lateral surface of a helical gear (***a***), stress distribution on Hertz's diagram at the pitch point of helical pair (***b***)

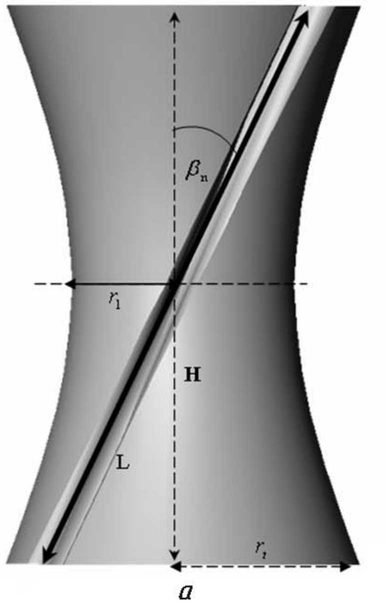

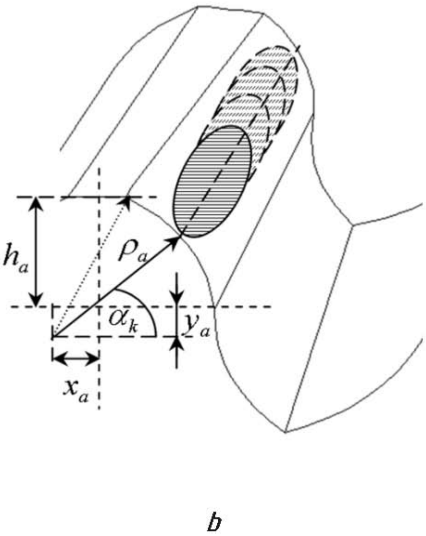

Fig. 3. For the definition of tooth length L (***a***) and arc length L_a (***b***)

For the purpose of defining major and minor semiaxes of the instantaneous contact ellipse (Fig. 2.a), generalized Hooke's law and Winkler's hypothesis are used [21, 1]. Therefore, the function of contact deformations is defined as follows:

$$D(x,y) = B(x,y)\sigma_H(x,y), \tag{13}$$

where: $B(x,y)$ is a resilience coefficient of the mating pair of teeth, mm^3/N (variable), $\sigma_H(x,y)$ is a contact stress function.

The contact stress function of helical gear teeth will be defined below.

Using (7), the contact stress at any point within the elliptical contour is defined through the maximum (normal) stress in the area center:

$$\sigma_H = P = P_{max}\frac{z}{c} = P_{max}\sqrt{1-\left(\frac{x}{a}\right)^2-\left(\frac{y}{b}\right)^2}\,. \tag{14}$$

The contact deformation function will look as follows:

$$D(x,y) = \frac{a^2}{2\rho}\sqrt{1-\left(\frac{x}{a}\right)^2-\left(\frac{y}{b}\right)^2} = \frac{b^2}{2R}\sqrt{1-\left(\frac{x}{a}\right)^2-\left(\frac{y}{b}\right)^2}\,. \tag{15}$$

Normal stress P_n will be defined through the stress P at any interior point of an elliptical contour as follows:

$$P_n = \int_S P dS = \frac{P_{max}}{c}\int_S z dS\,, \tag{16}$$

where: the volume of semi-ellipsoidal compression is the following:

$$\int_S z dS = \frac{2}{3}\pi a b c\,. \tag{17}$$

Substituting the value of the integral (17) into (16), the expression for the maximum normal contact stress in the area center will look as follows:

$$P_{max} = \sigma_{max} = \frac{3P_n}{2\pi a b} = \frac{1{,}5P_n}{S}\,. \tag{18}$$

It is evident from (18) that the maximum stress σ_{max} in the elliptical area center of resilient contact is 1.5 times greater than the average stress set by the formula:

$$\sigma_s = \frac{P_n}{\pi ab} = \frac{P_n}{S}\,. \tag{19}$$

Contact stress is not a linear function of the normal load P_n, and with an increase of P_n it grows slower. This can be explained by the fact that under the load P_n, the local resilient deformation of a small volume of metal takes place in the contact zone. As a result, the contacting teeth approach each other. The convergence occurs so that the teeth points, which lie outside the deformation zone, move by a certain value along the z-axis. Therefore, with increase of P_n, a and b increase and the area of instantaneous contact patch also grows (5), and hence contact stresses reduce.

For the purpose of defining the coefficient B as constant in equation (13), the actual diagram of stresses distribution $\sigma_H(x,y)$ over the elliptical contact patch (Fig. 2, b) will be replaced with diagram of mean stresses σ_s (20) equally distributed over the given contact patch.

Then, (18) takes the following form:

$$\sigma_{max} = \frac{3P_n}{2\pi a b} = \frac{3}{2}\sigma_s . \qquad (20)$$

After replacing the variable resilience coefficient B (x, y) in equation (13) with constant B, the equation looks as follows:

$$D(x,y) = B\sigma(x,y) . \qquad (21)$$

For the purpose of using the function (21), it is necessary to define the expression of resilience coefficient B. Therefore, first we will use the dependence which characterizes the relationship between the resilient movements (deformations) D of teeth and stresses arising in them, namely:

$$D_m = K_m \sigma_s{}^n , \qquad (22)$$

where: K_m is dimensional parameter, mm/MPa, n is a power exponent, equal to 0,7...0,8 [13, 24] (with regard to the point contact of objects we should proceed from the exponent n = 0,7).

Applied to the mating pair of teeth of gear and wheel, contact stress equation, based on the generalized Hooke's law, will look as follows [1]:

$$\begin{cases} \sigma_1 = \dfrac{(\varepsilon_{zy} + \nu_1 \varepsilon_{zx})E_1}{1-\nu_1^2}, \\ \sigma_2 = \dfrac{(\varepsilon_{zy} + \nu_2 \varepsilon_{zx})E_2}{1-\nu_2^2}, \end{cases} \qquad (23)$$

where: $\varepsilon_{zx} = \dfrac{\Delta L_{zx}}{L_x}$, $\varepsilon_{zy} = \dfrac{\Delta L_{zy}}{L_y}$ is relative deformations, ΔL_{zx}, ΔL_{zy} are absolute deformations, $L_x = 2a$, $L_y = 2b$ are lengths of contact ellipse axes, ν_1, ν_2 are Poisson coefficients, E_1, E_2 are resilience moduli of teeth materials.

Taking into account the equality $\Delta L_{zx} = \Delta L_{zy}$, we obtain the expression $\varepsilon_{zx} L_x = \varepsilon_{zy} L_y$, basing on which, in case of $L_x = 2a$, $L_y = 2b$, $\dfrac{a}{b} = \alpha$ (α is an ellipticity coefficient [6]), the next formulas will be obtained:

$$\frac{\varepsilon_{zy}}{\varepsilon_{zx}} = \frac{L_x}{L_y} = \frac{2a}{2b} = \frac{a}{b} = \alpha; \quad \varepsilon_{zy} = \alpha \varepsilon_{zx} .$$

Taking into account that $\Delta L_{zx} = \dfrac{a^2}{2\rho}$, then $\varepsilon_{zy} = \varepsilon_{zx}\alpha = \dfrac{\Delta L_{zx}}{L_x}\alpha = \dfrac{a^2}{2\rho 2a}\alpha = \dfrac{a}{4\rho}\alpha$, where $\rho = \dfrac{\rho_a \rho_f}{\rho_a + \rho_f}$ is a reduced radius of curvature of the lateral tooth profiles.

After placing the right side of the dependence $\varepsilon_{zy} = \alpha \varepsilon_{zx} = \dfrac{a}{4\rho}\alpha$ into the equations (23), they will look as follows:

$$\begin{cases} \sigma_1 = \dfrac{\varepsilon_{zx}(\alpha + \nu_1)E_1}{1-\nu_1^2} = \dfrac{a(\alpha + \nu_1)E_1}{4\rho(1-\nu_1^2)}, \\ \sigma_2 = \dfrac{\varepsilon_{zx}(\alpha + \nu_2)E_2}{1-\nu_2^2} = \dfrac{a(\alpha + \nu_2)E_2}{4\rho(1-\nu_2^2)}. \end{cases} \qquad (24)$$

Based on the dependence (22), when $n = 0.7$ and taking into account the expression

(24), two equations of resilient displacements of teeth mating pair will be defined as follows:

$$\begin{cases} D_1 = K_1\sigma_1^{0.7} = K_1\left(\dfrac{a(\alpha+\nu_1)E_1}{4\rho(1-\nu_1^2)}\right)^{0.7}, \\ D_2 = K_2\sigma_2^{0.7} = K_2\left(\dfrac{a(\alpha+\nu_2)E_2}{4\rho(1-\nu_2^2)}\right)^{0.7}. \end{cases} \quad (25)$$

From (25) and taking into account that $D = \Delta L_{zx} = a^2/(2\rho)$, the dependence of dimensional parameters will be defined as follows:

$$\begin{cases} K_1 = D_1\left(\dfrac{4\rho}{a}\dfrac{1-\nu_1^2}{(\alpha+\nu_1)E_1}\right)^{0.7} = \\ = \dfrac{a^2}{2\rho}\left(\dfrac{4\rho}{a}\right)^{0.7}\left(\dfrac{1-\nu_1^2}{(\alpha+\nu_1)E_1}\right)^{0.7} = \\ = 2^{0.4}\dfrac{a^{1.3}}{\rho^{0.3}}\left(\dfrac{1-\nu_1^2}{(\alpha+\nu_1)E_1}\right)^{0.7}, \\ K_2 = D_2\left(\dfrac{4\rho}{a}\dfrac{1-\nu_2^2}{(\alpha+\nu_2)E_2}\right)^{0.7} = \\ = \dfrac{a^2}{2\rho}\left(\dfrac{4\rho}{a}\right)^{0.7}\left(\dfrac{1-\nu_2^2}{(\alpha+\nu_2)E_2}\right)^{0.7} = \\ = 2^{0.4}\dfrac{a^{1.3}}{\rho^{0.3}}\left(\dfrac{1-\nu_2^2}{(\alpha+\nu_2)E_2}\right)^{0.7}. \end{cases} \quad (26)$$

Next, based on the relation (19) and expressions (26), the equations of contact resilience of gear and wheel teeth will be defined as follows:

$$\begin{cases} \delta_1 = \dfrac{D_1}{P_n} = \dfrac{K_1\sigma_s^{0.7}}{P_n} = \dfrac{2^{0.4}a^{1.3}}{\rho^{0.3}P_n}\left(\dfrac{1-\nu_1^2}{(\alpha+\nu_1)E_1}\right)^{0.7}\left(\dfrac{P_n\alpha}{\pi a^2}\right)^{0.7} = \\ = \dfrac{2^{0.4}}{\pi^{0.7}a^{0.1}(\rho P_n)^{0.3}}\left(\dfrac{\alpha(1-\nu_1^2)}{(\alpha+\nu_1)E_1}\right)^{0.7}, \\ \delta_2 = \dfrac{D_2}{P_n} = \dfrac{K_2\sigma_s^{0.7}}{P_n} = \dfrac{2^{0.4}a^{1.3}}{\rho^{0.3}P_n}\left(\dfrac{1-\nu_2^2}{(\alpha+\nu_2)E_2}\right)^{0.7}\left(\dfrac{P_n\alpha}{\pi a^2}\right)^{0.7} = \\ = \dfrac{2^{0.4}}{\pi^{0.7}a^{0.1}(\rho P_n)^{0.3}}\left(\dfrac{\alpha(1-\nu_2^2)}{(\alpha+\nu_2)E_2}\right)^{0.7}. \end{cases} \quad (27)$$

Taking into account the size of elliptical contact patch (5), equal to $S = \pi ab$, and relations (27). The resilience coefficient will be defined as follows:

$$B = S(\delta_1+\delta_2) = \pi a b(\delta_1+\delta_2) = \pi\frac{a^2}{\alpha}(\delta_1+\delta_2) =$$

$$= \pi\frac{a^2}{\alpha}\cdot\frac{2^{0.8}}{\pi^{0.7}a^{0.1}(\rho P_n)^{0.3}}\times$$

$$\times\left(\left(\frac{\alpha(1-\nu_1^2)}{(\alpha+\nu_1)E_1}\right)^{0,7} + \left(\frac{\alpha(1-\nu_2^2)}{(\alpha+\nu_2)E_2}\right)^{0,7}\right) = \frac{2^{0,8}a^{1,9}\pi^{0,7}}{(\alpha\rho P_n)^{0,3}}\times$$

$$\times\left(\left(\frac{1-\nu_1^2}{(\alpha+\nu_1)E_1}\right)^{0,7} + \left(\frac{1-\nu_2^2}{(\alpha+\nu_2)E_2}\right)^{0,7}\right). \quad (28)$$

According to the expression (28), the function (21) of teeth contact deformation will take the final form:

$$D(x,y) = \frac{2^{0,8}a^{1,9}\pi^{0,7}}{(\alpha\cdot\rho\cdot P_n)^{0,3}}\times$$

$$\times\left(\left(\frac{1-\nu_1^2}{(\alpha+\nu_1)E_1}\right)^{0,7} + \left(\frac{1-\nu_2^2}{(\alpha+\nu_2)E_2}\right)^{0,7}\right)\sigma(x,y). \quad (29)$$

On the basis of (16) and (29), taking into account (15), the equation that characterizes the stressed deformed state of the teeth mating pair will look as follows:

$$BP_n = B\int_S P\,dS = B\int_{-b}^{b}\int_{-a}^{a}\sigma(x,y)dxdy =$$

$$= \frac{2^{0.8}a^{1.9}\pi^{0.7}P_n}{(\alpha\cdot\rho\cdot P_n)^{0.3}}\left(\left(\frac{1-\nu_1^2}{(\alpha+\nu_1)E_1}\right)^{0,7} + \left(\frac{1-\nu_2^2}{(\alpha+\nu_2)E_2}\right)^{0,7}\right) =$$

$$= \frac{a^2}{2\rho}\int_{-b}^{b}\int_{-a}^{a}\sqrt{1-\left(\frac{x}{a}\right)^2-\left(\frac{y}{b}\right)^2}\,dxdy =$$

$$= \frac{a^2}{2\rho}\cdot\frac{2}{3}\pi ab = \frac{\pi a^3 b}{3\rho} = \frac{\pi a^4}{3\alpha\rho}. \quad (30)$$

This equation will be transformed to the following:

$$a^{2,1} = 2^{0,8} \cdot 3 \cdot \frac{(\alpha\rho P_n)^{0,7}}{\pi^{0,3}} \times$$
$$\times \left(\left(\frac{1-\nu_1^2}{(\alpha+\nu_1)E_1} \right)^{0,7} + \left(\frac{1-\nu_2^2}{(\alpha+\nu_2)E_2} \right)^{0,7} \right). \quad (31)$$

Exponentiating the left and right parts of the last equation to power 10/21, the small semiaxis of the ellipse will be defined:

$$a = 1{,}8658 \times$$
$$\times \sqrt[3]{\left(\left(\frac{\alpha\rho P_n(1-\nu_1^2)}{(\alpha+\nu_1)E_1} \right)^{0,7} + \left(\frac{\alpha\rho P_n(1-\nu_2^2)}{(\alpha+\nu_2)E_2} \right)^{0,7} \right)^{\frac{10}{7}}}. \quad (32)$$

Based on dependence (32), the major semiaxis of the elliptical contact patch will be defined as follows:

$$b = \frac{a}{\alpha} = \frac{1{,}8658}{\alpha} \times$$
$$\times \sqrt[3]{\left(\left(\frac{\alpha\rho P_n(1-\nu_1^2)}{(\alpha+\nu_1)E_1} \right)^{0,7} + \left(\frac{\alpha\rho P_n(1-\nu_2^2)}{(\alpha+\nu_2)E_2} \right)^{0,7} \right)^{\frac{10}{7}}}. \quad (33)$$

Then, (5) will be transformed to:

$$S = \pi \frac{3{,}478}{\alpha} \times$$
$$\times \sqrt[3]{\left(\left(\frac{\alpha\rho P_n(1-\nu_1^2)}{(\alpha+\nu_1)E_1} \right)^{0,7} + \left(\frac{\alpha\rho P_n(1-\nu_2^2)}{(\alpha+\nu_2)E_2} \right)^{0,7} \right)^{\frac{20}{7}}}. \quad (34)$$

And finally, taking into account (34), the contact tightness coefficient (12) will look as follows:

$$K_p = \frac{S}{S_z} = \frac{\pi ab \sin\beta_n}{2\rho_a \sqrt{r_t^2 - r_1^2} \left(arcsin\left(\frac{h_a + y_a}{\rho_a} \right) - arcsin\left(\frac{y_a}{\rho_a} \right) \right)} =$$

$$= \frac{3{,}478 \cdot \pi \sin\beta_n \sqrt[3]{\left(\left(\frac{\alpha\rho P_n(1-\nu_1^2)}{(\alpha+\nu_1)E_1} \right)^{0,7} + \left(\frac{\alpha\rho P_n(1-\nu_2^2)}{(\alpha+\nu_2)E_2} \right)^{0,7} \right)^{\frac{20}{7}}}}{\alpha\rho_a \sqrt{r_t^2 - r_1^2} \left(arcsin\left(\frac{h_a + y_a}{\rho_a} \right) - arcsin\left(\frac{y_a}{\rho_a} \right) \right)}. \quad (35)$$

As a matter of practice, in the calculations: $\nu_1 = \nu_2 = \nu = 0{,}3$, and $E_1 = E_2 = E$. Based on this, the equation (32) will be simplified:

$$K_p = \frac{6{,}73 \cdot \pi \sin\beta_n \sqrt[3]{\left(\frac{\alpha\rho P_n(1-\nu^2)}{(\alpha+\nu)E} \right)^2}}{\alpha\rho_a \sqrt{r_t^2 - r_1^2} \left(arcsin\left(\frac{h_a + y_a}{\rho_a} \right) - arcsin\left(\frac{y_a}{\rho_a} \right) \right)}. \quad (36)$$

Next, the influence of gear parameters on contact tightness coefficient (36) will be studied (Fig. 4 – Fig. 7).

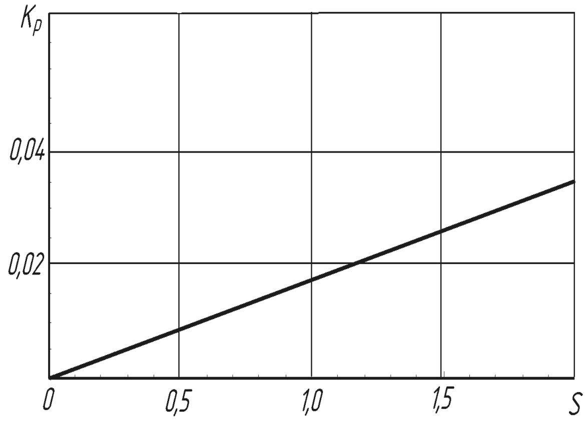

Fig. 4. Dependency K_p (contact tightness coefficient) on S (contact area of the lateral tooth surface)

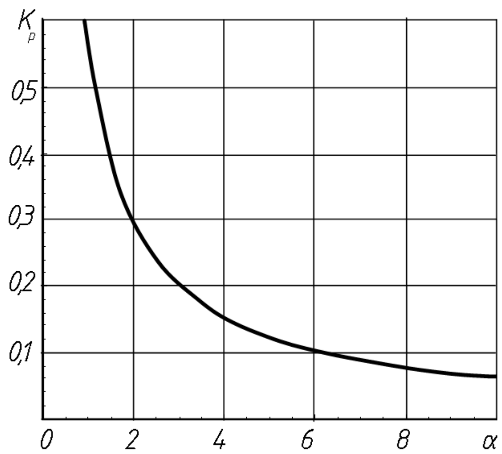

Fig. 5. Dependency K_p (contact tightness coefficient) on α (ellipticity)

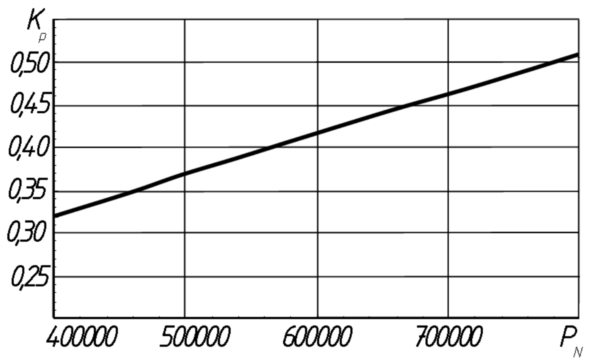

Fig. 6. Dependency K_p (contact tightness coefficient) on P_N (normal stress in nominal contact point)

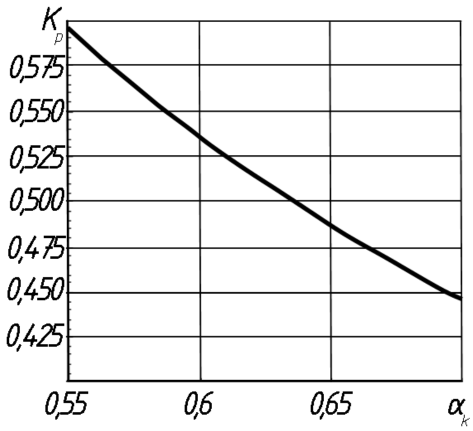

Fig. 7. Dependency K_p (contact tightness coefficient) on α_k (pressure angle in nominal contact point)

In Fig. 4–7, it is evident that increasing P_N (normal stress in nominal contact point) or increasing S (instantaneous contact patch area), which can be the consequence of increasing in P_N, the value of contact tightness coefficient is increased and, therefore, the load capacity increases, and the conditions of oil-film wedge formation are improved, friction decreases, transmission performance improves, contact and bending stress decreases.

Therefore, it can be justly concluded that gear load capability is in direct dependence on the contact tightness coefficient, which should be classified as the criterion for selecting of tooth rim parameters from the point of view of the best durability characteristics.

CONCLUSIONS

1. The main factors affecting the performance and competitiveness of crossed-axis helical gear were studied. Theoretical research on building up a mathematical model of helical gear teeth loaded state was conducted.
2. Analytical dependences of contact tightness coefficient on load factors and geometric parameters of original profile and original hyperboloid surfaces were defined. The considered factor belongs to the main group of criteria included in the objective function that is used for the multi-criteria synthesis of a new initial gear profile.
3. Analytical dependences were derived that uniquely identify the theoretical initial surfaces of helical gears.
4. With the aim of defining a correlation dependence between performance criteria, a multiple correlation analysis of qualitative variable was conducted. This will enable setting up a close correlation between the contact tightness coefficient and load capacity and teeth contact strength. The obtained results of the comparative analysis confirmed the accuracy of the developed theory and the adequacy of the proposed mathematical models.

REFERENCES

1. **Andreev A.V., 1981.:** Calculation of details under complex stress state. – M.: Mashinostroenie, , 215. (in Russian).
2. **Belodedov V., Nosko P., Fil P., 2010.:** Selection of optimal parameters dosator with horizontal dick in the general criterion. – Lublin, "Teka", V. XC, 19-27.
3. **Belodedov V., Nosko P., Fil P., Mazneva M., Boyko G., 2010.:** Selection of batchen with horizontal dick parameters while maize sowing. – Lublin, "Teka", V. XA, 33-40.
4. **Belodedov V., Nosko P., Fil P., Stavicky V., 2007.:** Parameter optimization using coefficient of variation of intervals for one-seed sowing apparatus with horizontal disc during maize seeding. – Lublin, "Teka". vol.7, 31-37.
5. **Belodedov V., Velichko N., Fil P., Breshev V., Mazneva M.. 2008.:** "Simulation of influence of seeding conditions on closed to calculated quantity". – Lublin, "Teka", V. 10A, 11-17.
6. **Demidov S., 1979.:** The theory of elasticity. – M., «Higher school». 432.

7. Design of bevel and hypoid gears. – “Glisson” company instructions (USA). – M. – 2001, 274. (in Russian).
8. **Gribanov V.M., Medintseva Y.V., Ratov D.V., 2010.:** Novikov’s gears. Accuracy problems. – Lugansk “Knowledge”, 252.
9. **Gribanov V.M., Medintseva Y.V., Ratov D.V., 2010.:** On production of quasi-hyperboloid gears. – Bulletin of Volodymyr Dahl East Ukrainian National University. Lugansk, 12 (154), Vol. 2, 236 – 239. (in Russian).
10. **Gribanov V., Ratov D., Balitskaya T., 2009.:** Imitating modeling hyperboloid gears. – Lublin, "Teka", V. XC, 54-61.
11. **Grybanov V.M., 2003.:** Theory of hyperboloid gears. – Lugansk, Volodymyr Dahl East Ukrainian National University, 272. (in Russian).
12. **Ivanov M., 1981.:** Wave gearings. – M.: Higher school. 184.
13. **Levina Z.M., Reshetov D.N., 1971.:** Contact stiffness of machines. – M.: Mashinostroenie, 264. (in Russian).
14. **Litvin F., 1968.:** Theory of gearings. – M: Science. 584.
15. **Medintseva Y.V., Ratov D.V.** On the accelerated sliding rate of helical gear trains. – Lugansk. Bulletin of Lugansk National Agricultural University. Engineering Sciences, 76 (99), 55-61. (in Russian).
16. **Medintseva Y.V., Ratov D.V., Balytska T.Y.** 2007.: Numerical multicriteria synthesis of Novikov gears with two lines coupling. // Bulletin of Volodymyr Dahl East Ukrainian National University, No. 12 (118), Vol. 1, 52-56. (in Russian).
17. **Nosko P., Shishov V., Fil P., Muhovatiy A., Sklyar U., 2008.:** Parametrical optimization of worm gears on losses in gearing. TEKA Commission of Motorization and Power Industry in Agriculture. – Lublin. – V. VIII. 213-221.
18. **Nosko P., Shishov V., Tkach P., Sklyar U., 2010.:** Gearing with increased teeth wear. TEKA Commission of Motorization and Power Industry in Agriculture. – Lublin. – V. XB. 87-94.
19. **Novikov M.L., 1958.:** Gear trains with new coupling engagement. – M.: Zhukovsky AFEA, 186. (in Russian).
20. **Pavlenko A.V., Fediakin R.V., Chesnokov V.A., 1978.:** Gear train with Novikov’s gearing. – Kiev: “Tehnika”, 144. (in Russian).
21. **Popov A.P., 2008.:** Contact strength of gear mechanisms. – Nikolaev.: NUK. (in Russian).
22. **Popov A.P., Selivanovskyi V.Y., 2003.:** New method for calculating contact stresses in Novikov’s gearing. – Kharkov, Bulletin of National Technical University “KhPI”, (8), 82-87. (in Russian).
23. **Pysarenko G.S., 1979.:** Strength of materials. Textbook for high schools. Edit. by Pysarenko. – Kiev, 696 (in Russian).
24. **Ryzhov E.V., 1946.:** Contact stiffness of machine parts. CNIITMASH. – M. (in Russian).
25. **Shyshov V.P., Nosko P.L., Velychko N.I., Karpov A.P., 2009.:** Highly loaded helical gears. – Lugansk. Volodymyr Dahl East Ukrainian National University, 240. (in Russian).
26. **Strelnikov V., 2000.:** Determination of forces acting on flexible gear on wave generator side // Bulletin of Kharkov National Pedagogical University. - Kharkov. – Issue 109. 154-158.
27. **Strelnikov V., 2000.:** Interaction between wave generator and flexible gear // Advanced technologies and engineering systems. International edited volume – Donetsk: Donetsk State Technical University. – Issue 13. 191 – 199.
28. **Strelnikov V., Sevostyanov S., 1998.:** About energy losses in wave gearing meshing // Protection of metallurgical machines against failures. – Issue No.3. 237 – 241.
29. **Strelnikov V., Sevostyanov S., 1999.:** Determination of energy losses in wave-type gear reducers for metallurgical and mining equipment// Metallurgy and mining industry. – No.5. 102-105.
30. **Strelnikov V., Sevostyanov S., 1999.:** Determination of energy losses in wave-type gear reducers for metallurgical and mining equipment// Metallurgy and mining industry. – No.5. 102-105.
31. **Strelnikov V., Sevostyanov S., 2000.:** Determination of axial forces on wave gearing flexible gear // Bulletin of Kharkov National Pedagogical University. - Kharkov. – Issue 109. 159-172.

КРИТЕРИЙ НАГРУЗОЧНОЙ СПОСОБНОСТИ ЗУБЧАТЫХ ВИНТОВЫХ ПЕРЕДАЧ

Павел Носко, Валентин Шишов, Денис Ратов, Павел Филь, Андрей Лысенко

Аннотация. Представлены результаты исследований повышения нагрузочной способности и введен в рассмотрение один из важных критериев работоспособности передач — коэффициент плотности прилегания активных боковых поверхностей зубьев винтовых передач, характеризующий напряженное состояние зубьев винтовой передачи. Получены аналитические зависимости, однозначно определяющие теоретические начальные поверхности винтовых передач.
Результатами сравнительного анализа подтверждена прямая зависимость несущей способности зубчатой передачи от рассмотренного коэффициента плотности прилегания.
Ключевые слова: винтовая передача, коэффициент плотности прилегания, критерий нагрузочной способности, целевая функция, оптимизация, синтез, начальные поверхности, аксоиды.